Vol. 36 (2005) ACTA PHYSICA POLONICA B No 10

# ON MULTISTEP DIRECT EMISSION OF ONE AND TWO NUCLEONS AND THE GRADUAL ABSORPTION THAT FOLLOWS

Andrzej Marcinkowski

The Andrzej Sołtan Institute for Nuclear Studies
Hoża 69, 00-681 Warszawa, Poland
Andrzej.Marcinkowski@fuw.edu.pl

(Received May 20, 2005)

The multistep direct reaction theory of Feshbach, Kerman and Koonin (FKK) is used with the enhanced non-DWBA matrix elements and with both the coherent vibrations and the incoherent particle–hole excitations, included. Distinction between bound and unbound final particle–hole states is made, since only the former determine genuine one-step cross sections that observe the energy weighted sum rule limits and can be convoluted to obtain the multistep cross sections for emission of one particle. The cross sections to unbound final states describe more complicated direct processes. Only the very specific of such processes can be evaluated in terms of the FKK theory. These novelties are verified in analyses of a representative series of reactions.

PACS numbers: 25.40.Fq, 25.40.Ep, 25.40.Kv, 24.60.Gv

## 1. Introduction

The concept of statistical multistep collisions [1] is common in quantum mechanical descriptions of the mechanism of the pre-equilibrium nuclear reactions in the continuum [2–4]. Especially the nucleon induced reactions have been widely described by the theory of Feshbach, Kerman and Koonin (FKK) [2], who distinguished between the multistep direct (MSD) reactions that involve a chain of states of increasing complexity, each including only one virtual unbound particle, and the multistep compound (MSC) reactions involving a chain of quasi-bound states that develop towards the compound nucleus. In the following only the former MSD reactions are discussed, although the two reaction chains are not independent but linked together by transitions that damp the unbound particles of low energy into the compound states at each reaction stage. The damping transitions give rise to gradual absorption [5] instead of the one-step absorption into the quasi-bound $2p1h$ doorway states [2]. On the other hand, gradual absorption to be effective requires enhanced transition matrix elements originally included in the FKK theory [6,7]. Both the gradual absorption and the enhanced MSD reactions reflect the interference of the strong nonelastic direct processes with the intensive compound nucleus background [8]. The FKK theory allows of only one particle in the continuum and therefore it can describe only one-particle emission. The calculation of the cross sections for the one-step, one-particle emission is described in Chapters 2 and 3. In Chapter 4 the multistep cross sections follow. In Chapter 5 it is shown that some very specific ones of the more complicated direct processes, *e.g.* two-particle emission followed by multistep scattering or one-particle emission associated with the damping of the other continuum particle, can be evaluated in the framework of FKK [9,10].

## 2. The one-step direct emission of one particle

Recently it was found that in case of low multipolarities $\lambda{=}L{\leq}4$ , the correlations that bring the particle–hole ($ph$) pairs into a collective motion dominate over the incoherent spatial motions, contrary to the $ph$ pairs with $L{>}4$ that are governed by the incoherent spatial motions. This finding, which followed the analysis of the cross sections in terms of the energy weighted sum rules (EWSR's) [11,12], led to the following expression for the cross section of a one-step direct reaction to both the bound and the unbound final states [12–14]

$$1\mathrm{SD} = \sum_{\lambda\leq 4}^{\mathrm{one-phonon}} \sigma_\lambda(vib) + \sum_{L>4} \sigma_L(ph)\,. \tag{1}$$

Later, the incoherent excitations of the bound $ph$ states were distinguished from the unbound ones, and this resulted in a suitable formula for the cross section of one-step emission of one particle leading to the excitation of bound final states only [10,15],

$$1\mathrm{SD}_{\mathrm{bound}} = \sum_{\lambda\leq 4}^{\mathrm{one-phonon}} \sigma_\lambda(vib) + \sum_{L>4}^{\mathrm{one-step}} \sigma_L(ph)_{\mathrm{bound}}\,. \tag{2}$$

The latter is a genuine one-step, one-particle cross section that observes the EWSR's limits and is appropriate for folding into the multistep direct cross sections ($\mathrm{MSD_{bound}}$) of the FKK theory. Both the collective and the incoherent double-differential $ph$ cross sections in Eq. (2), are expressed in terms of the DWBA angular distributions by,

$$\sigma_\lambda(vib) = \sum_{n_{\lambda,\tau=0,1}} e_{\mathrm{a,b}} \times \beta^2_{n_{\lambda,\tau}} \left(\frac{J_{0,\tau}}{\mathrm{J}_{0,0}}\right)^2 \times \left(\frac{d\sigma}{d\Omega}\right)^{\mathrm{DWBA-macr}}_{n_{\lambda,\tau}} \times f[\hbar\omega_{n_{\lambda,\tau}}, \Gamma]\,, \qquad (3)$$

with $U_{0,\tau}/U_{0,0} = J_{0,\tau}/J_{0,0}$, and the ratio of the volume integrals of the terms in the nucleon–nucleon effective interaction $J_{0,1}/J_{0,0} \approx 1/2$. The quantity $e_{\mathrm{a,a}} = 1$ for nucleon scattering and $e_{\mathrm{a,b}} = 2$ for charge-exchange reactions [16], and

$$\sigma_L(ph)_{\mathrm{bound}} = \sum_{\mathrm{a,b}} (2L+1) \times \rho_{1p_{\mathrm{a}}1h_{\mathrm{b}}}(U, P, L, B_{\mathrm{a}}, \epsilon^{\mathrm{b}}_{\mathrm{F}}) \times V^2_{\mathrm{a,b}} \left\langle \left(\frac{d\sigma}{d\Omega}\right)^{\mathrm{DWBA-micr}}_{1p_{\mathrm{a}}1h_{\mathrm{b}}} \right\rangle . \qquad (4)$$

Here, both indices a and b denote either a neutron (n) or a proton (p). Thus, the sum in (4) includes two terms that describe nucleon scattering to the neutron particle–hole, $1p_{\mathrm{n}}1h_{\mathrm{n}}$, and the proton-particle–hole, $1p_{\mathrm{p}}1h_{\mathrm{p}}$, final states. In case of a charge-exchange reaction, the sum in (4) includes only one term corresponding to, either the mixed neutron-particle–proton-hole, $1p_{\mathrm{n}}1h_{\mathrm{p}}$, or the proton-particle–neutron-hole, $1p_{\mathrm{p}}1h_{\mathrm{n}}$, final states [12].

The macroscopic DWBA angular distributions in Eq. (3) are calculated with the form factors ff= $-R\partial U_{0,0}/\partial R$ obtained from the deformed optical potential. For nucleon scattering, the summations in Eqs. (1) to (3) practically extend over the known isoscalar $n_{\lambda,0}$, one-phonon $2^+$, $3^-$ and $4^+$ final states with $\beta_{n_{\lambda,0}}$, the phenomenological deformation parameters, see *e.g.* [15]. The dipole (GDR), quadrupole (GQR) and low energy component of the octupole (LEOR) giant resonances are also included. The LEOR exhausts 30% of the total octupole strength [17]. The strengths of the resonances are obtained by depleting the EWSR's. $f_\lambda$ is the energy distribution function, assumed to be Gaussian with a width adjusted to the experimental energy resolution for the low-energy levels, or Lorentzian with a width typical of the giant resonances. In case of a charge-exchange reaction, the deformation parameters $\beta_{n_{\lambda,1}}$ of the low energy collective levels in Eq. (3) are usually unknown, since these levels are weakly populated, except for the isobaric analogue state. Therefore, we assume that the collective excitations are dominated by the isovector giant resonances which, except for the dipole resonance, have widths of 10 MeV or more [17]. These wide collective structures are approximated by the smooth $\sigma_L(ph)_{\mathrm{bound}}$ cross sections calculated with $\lambda{=}L{\leq}\,4$. The resulting smooth cross sections are subsequently reduced according to the EWSR's limits [15,18], see also Chapter 3.

The microscopic DWBA angular distributions in (4) are calculated with a real effective interaction of Yukawa form with 1 fm range and strength reduced to unity. The standard values of the strength $V_{\rm p,p} = V_{\rm n,n} = 12.7$ MeV and $V_{\rm p,n} = V_{\rm n,p} = 43.1$ MeV are used [19] and their dependence on the incident energy is accounted for [20]. The microscopic cross sections are averaged over the final particle–hole states $(j_p j_h^{-1})_{LM}$ of the shell model [21] contained in 1 MeV intervals. However, when no states with given $L$ are found in the 1 MeV bin, the latter is increased until the state is found. This allows one also to use the standard DWBA code DWUCK-4 [22] to obtain approximate cross sections to final continuum states by making the unbound particle quasi-bound. Both the macroscopic and the microscopic cross sections are calculated with the DWUCK-4 code. The spectroscopic amplitude $(2j_h{+}1)^{1/2}$ is used in the microscopic option of DWUCK-4.

The level density $\rho_{1p_{\rm a}1h_{\rm b}}$ in (4) reads,

$$\rho_{1p_{\rm a}1h_{\rm b}}(U,P,L,B_{\rm a},\varepsilon_{\rm F}^{\rm b}) = P\times R_{1,1}(L)\times\omega_{1p_{\rm a}1h_{\rm b}}(U,B_{\rm a},\varepsilon_{\rm F}^{\rm b})\,, \qquad (5)$$

where $P = 1/2$ is the parity distribution and $R_{1,1}(L)$ the usual angular momentum distribution of Wigner type with the spin cut-off parameter $\sigma^2 = 0.56A^{2/3}$ [23]. The bound particle–hole state density $\omega_{1p_{\rm a}1h_{\rm b}}(U,B_{\rm a},\varepsilon_{\rm F}^{\rm b})$ is taken from [24],

$$\begin{aligned}\omega_{1p_{\rm a},1h_{\rm b}}(U,B_{\rm a},\varepsilon_{\rm F}^{\rm b}) \;=\; & g_{\rm a}g_{\rm b}[U-(U-B_{\rm a})\Theta(U-B_{\rm a})-(U-\varepsilon_{\rm F}^{\rm b})\Theta(U-\varepsilon_{\rm F}^{\rm b}) \\ & +(U-B_{\rm a}-\varepsilon_{\rm F}^{\rm b})\Theta(U-B_{\rm a}-\varepsilon_{\rm F}^{\rm b})]\,, \qquad (6)\end{aligned}$$

with $\rm a = b = p$ for $p_{\rm p} = h_{\rm p} = 1$ and $p_{\rm n} = h_{\rm n} = 0$; $\rm a = b = n$ for $p_{\rm n} = h_{\rm n} = 1$ and $p_{\rm p} = h_{\rm p} = 0$; $\rm a = n, b = p$ for $p_{\rm n} = h_{\rm p} = 1$ and $p_{\rm p} = h_{\rm n} = 0$; $\rm a = p, b = n$ for $p_{\rm p} = h_{\rm n} = 1$ and $p_{\rm n} = h_{\rm p} = 0$. The state density of (6) is restricted to particle energies below the binding energy $B_{\rm a}$ and hole energies that do not exceed the Fermi energy $\varepsilon_{\rm F}^{\rm b}$, with $\Theta$ being the Heaviside step function. The standard equidistant single-particle state densities for protons, $g_{\rm p} = Z/13$, and neutrons, $g_{\rm n} = N/13$, are used. Taking $P{=}1/2$ is an approximation that implies the contributions from spin–flip ($\Delta s{=}1$) transitions to be negligible [25]. In this way, it is possible to compensate for the fact that in the above-mentioned averaging of microscopic DWBA angular distributions over final $ph$ states of the shell model (the angular brackets in Eq. (4)), only the non-spin-flip ($\Delta s = 0$) reactions to natural parity states are considered.

In the state density $\omega_{1p_\mathrm{a}1h_\mathrm{b}}$ in the second r.h.s. term of Eq. (1), the restriction of particle energies below the binding energy is removed [26,27],

$$\omega_{1p_\mathrm{a},1h_\mathrm{b}}\left(U,\varepsilon_\mathrm{F}^\mathrm{b}\right) = g_\mathrm{a}g_\mathrm{b}\left[U-(U-\varepsilon_\mathrm{F}^\mathrm{b})\Theta\left(U-\varepsilon_\mathrm{F}^\mathrm{b}\right)\right] . \tag{7}$$

The indices a and b are the same as in (6).

The isospin is omitted in the incoherent *ph* cross sections of (1), (2) and (4), which implies complete isospin mixing. This assumption may not be adequate at incident energies around 100 MeV, although a likely impact of isospin within the FKK approach is assessed to be small [25].

## 3. The one-step cross sections in terms of the EWSR's

The one-phonon collective vibrations of energy $\varepsilon_{n_{\lambda,\tau}}$ (including the giant resonances) observe the EWSR's by definition, *i.e.*

$$\sum_{n_{\lambda,\tau}}^{\mathrm{one-phonon}} \varepsilon_{n_{\lambda,\tau}} \times \beta^2_{n_{\lambda,\tau}} \;=\; S_{\lambda,\tau} \ , \tag{8}$$

where $S_{0,0} = 10\pi\hbar^2/(3mAR^2)$ for monopole, $S_{1,1} = \pi\hbar^2/(2mNZR^2)$ for dipole and $S_{\lambda\geq 2,\tau} = S_{L\geq 2} = 2\pi\hbar^2 L(2L+1)/(3mAR^2)$ for multipole phonons [28].

To evaluate the incoherent cross sections, the method of Tamura *et al.* [3] is applied. These authors have shown that the microscopic DWBA form factors, averaged over a number of shell model *ph* pairs, always peak at the nuclear surface and therefore may be approximated by the derivative of the optical potential as in analyses of inelastic scattering to low-energy collective states. This enables us to assign an equivalent strength parameter $\hat{\beta}_{L,\tau}$ to the cross section for the incoherent excitation of *ph* pairs of given $L$ and energy [29]. By integrating the calculated $\sigma_L(ph)_\mathrm{bound}$ cross sections within $\Delta U$=1 MeV bins for each $L$>4, one extracts the $\hat{\beta}_{L,\tau}$ in accordance with the macroscopic DWBA model,

$$\int\limits_U^{U+\Delta U}\int \sigma_L(ph)_\mathrm{bound} d\Omega dU = \sum_{\tau=0,1} e_{\mathrm{a,b}} \times \hat{\beta}^2_{L,\tau}\left(\frac{\mathrm{J}_{0,\tau}}{\mathrm{J}_{0,0}}\right)^2 \times \int \left(\frac{d\sigma}{d\Omega}\right)^{\mathrm{DWBA-macr}}_{L,U+\frac{1}{2}\Delta U} d\Omega \ , \tag{9}$$

for the fictitious states corresponding to an energy of $U + \Delta U/2$ in each successive 1 MeV bin [11,12]. The strength parameters obtained from (9) are then subjected to the sum rule limits $S_{L,\tau}$ as follows

$$\begin{aligned}&\sum_{U=0}^{E_{\rm inc}+Q-1}\left(U+\frac{1}{2}\Delta U\right)\sum_{\tau=0,1}e_{\rm a,b}\times\hat{\beta}^2_{L,\tau}\left(\frac{\rm J_{0,\tau}}{\rm J_{0,0}}\right)^2\\&=R_L\times e_{\rm a,b}\sum_{\tau=0,1}\left(\frac{\rm J_{0,\tau}}{\rm J_{0,0}}\right)^2\times S_{L,\tau}\,.\end{aligned}\tag{10}$$

*E.g.* for nucleon scattering,

$$\sum_{U=0}^{E_{\rm inc}-1}\left(U+\frac{1}{2}\Delta U\right)\left(\hat{\beta}^2_{L>4,0}+0.25\hat{\beta}^2_{L>4,1}\right)=R_L\times 1.25S_{L>4}\,,\tag{11}$$

and for charge-exchange reactions,

$$\sum_{U=0}^{E_{\rm inc}+Q-1}\left(U+\frac{1}{2}\Delta U\right)\times\hat{\beta}^2_{L>4,1}=R_L\times S_{L>4}\ .\tag{12}$$

In practice, the calculated one-step cross sections to the bound $1p1h$ states observe the limits for $L>4$, provided that $R_L\leq 2$ allowing for the approximate nature of the EWSR's limits [30].

The parameters $\hat{\beta}_{L\leq 4,1}$, obtained from (9) with the smooth $\sigma_{L\leq 4}(ph)_{\rm bound}$ cross sections are also subjected to the EWSR's limits $S_{L\leq 4}$ in (12). It is worth recalling that the smooth cross sections are used to approximate the isovector collective $\sigma_{\lambda\leq 4}(vib)$ term, in Eqs. (1) and (2), in the case of the charge-exchange reaction stages (pn) or (np), (see Chapter 2). In this case the reduction factors $R_L^{-1}$ are applied to both sides of (12).

## 4. The multistep direct emission of one particle

The multistep cross sections of the FKK theory are obtained by multiple folding of the one-step cross sections [2,31],

$$\begin{aligned}{\rm MSD_{bound}}\ =&\int\frac{m_1E_1}{(2\pi)^2\hbar^2}dE_1{\rm d}\Omega_1...\int\frac{m_{M-1}E_{M-1}}{(2\pi)^2\hbar^2}dE_{M-1}d\Omega_{M-1}\\&\times\left(1{\rm SD_{bound}}\right)_M\times{\rm S}^{-2}\left(1{\rm SD_{bound}}\right)_{M-1}...{\rm S}^{-2}\left(1{\rm SD_{bound}}\right)_1\ .\end{aligned}\tag{13}$$

$E_{M-1}$ and $m_{M-1}$ are the energy and mass of the scattered nucleon after the $M$-th stage of the reaction. The final states in the $(ph)$ components of the $1{\rm SD_{bound}}$ cross sections in Eq. (13) are assumed to be $1p1h$ states independent of the reaction stage $M$. Thus, all $ph$ pairs excited at the reaction stages preceding stage $M$ act as spectators only. On the other hand, each phonon in the ($vib$) cross section in Eq. (13) results in multi-phonon states [32] built on the final phonon states of the preceding reaction stage. The energies of the multi-phonon states are sums of energies of the constituent phonons. Therefore, it is important to include into the ($vib$) component only one-phonon states. The successive double-differential cross sections $(1\mathrm{SD}_{\mathrm{bound}})_{M-1}$, except the last $M$-th one are enhanced due to the biorthogonality of the outgoing distorted waves $< \hat{\chi}^{(+)} | = \mathrm{S}^{-1} < \chi^{(-)} |$ in the non-normal DWBA matrix elements [6]. For a given outgoing distorted wave $\ell_{M-2}$, in the incident channel and orbital angular momentum transfer $L$, a number of partial waves $\ell_{M-1}$ (triangle rule) contribute to the incoming distorted waves in the outgoing channel. The latter waves are enhanced by the corresponding $\mathrm{S}^{-1}_{\ell_{M-1}}$. The elastic scattering matrix elements $\mathrm{S}_{\ell_{M-1}}$ are related to the partial wave transmission coefficients $T_\ell$ of the optical potential, $\mathrm{S}^2_{\ell_{M-1}}{=}1{-}T_{\ell_{M-1}}$ [33]. The enhanced transition matrix elements are averaged over energy [12,34]. The overall effect of the energy averaging is approximated by using an effective average enhancing factor $\langle \mathrm{S}_L^{-1}\rangle$ acting on all partial waves $\ell_{M-1}$ for a specific $L$. The average $\langle \mathrm{S}_L^{-1}\rangle$ is free of the fluctuations or singularities that arise at the energies of the single particle resonances, where $T_L \approx 1$. The averaged enhancing factors apply not only to the excitation of the incoherent $ph$ pairs but also to those that add coherently to a collective vibration, since the distorted waves $< \chi^{(+)} |$, whether the excited states are single-particle ones or collective, are the same eigenfunctions of the complex optical potential and form a complete set with the adjoint distorted waves $\langle \hat{\chi}^{(+)} |$. Thus, according to Eq. (2), the $(M{-}1)$ out of the $M$ $1\mathrm{SD}_{\mathrm{bound}}$ cross sections in equation (13), contain a sum of the enhanced $(\mathrm{S}^{-2}vib) = \sum_{\lambda\leq 4}\langle \mathrm{S}_\lambda^{-1}\rangle^2\sigma_\lambda(vib)$ and $(\mathrm{S}^{-2}ph_{\mathrm{b}}){=}\sum_{L>4}{<}\mathrm{S}_L^{-1}{>}^2\sigma_L(ph_{\mathrm{b}})$ cross sections. As a result, the multistep cross section of equation (13) contains the following combinations of the above two terms [13,35]:

$1\mathrm{SD}_{\mathrm{bound}}$, $(vib) + (ph_{\mathrm{b}})$ ,
$2\mathrm{SD}_{\mathrm{bound}}$, $(\mathrm{S}^{-2}vib, vib) + (\mathrm{S}^{-2}ph_{\mathrm{b}}, vib) + (\mathrm{S}^{-2}vib, ph_{\mathrm{b}}) + (\mathrm{S}^{-2}ph_{\mathrm{b}}, ph_{\mathrm{b}})$,
$3\mathrm{SD}_{\mathrm{bound}}$, $(\mathrm{S}^{-2}vib, \mathrm{S}^{-2}vib, vib) + (\mathrm{S}^{-2}ph_{\mathrm{b}}, \mathrm{S}^{-2}vib, vib) + (\mathrm{S}^{-2}vib, \mathrm{S}^{-2}ph_{\mathrm{b}}, vib)$
$+ (\mathrm{S}^{-2}vib, \mathrm{S}^{-2}vib, ph_{\mathrm{b}}) + (\mathrm{S}^{-2}ph_{\mathrm{b}}, \mathrm{S}^{-2}ph_{\mathrm{b}}, vib) + (\mathrm{S}^{-2}ph_{\mathrm{b}}, \mathrm{S}^{-2}vib, ph_{\mathrm{b}})$
$+ (\mathrm{S}^{-2}vib, \mathrm{S}^{-2}ph_{\mathrm{b}}, ph_{\mathrm{b}}) + (\mathrm{S}^{-2}ph_{\mathrm{b}}, \mathrm{S}^{-2}ph_{\mathrm{b}}, ph_{\mathrm{b}})$,
$4\mathrm{SD}_{\mathrm{bound}}$, *etc.*,

where for simplicity the summations over $\lambda{=}L$ are omitted and the index b stands for "bound".

When distinction between proton or neutron leading particle in the continuum is made, a number of different sequences of one-step reaction stages can contribute to a given $\mathrm{MSD}_{\mathrm{bound}}$ reaction [25]. In order to reduce the number of terms describing the $\mathrm{MSD}_{\mathrm{bound}}$ cross section the $(\mathrm{S}^2 vib)_{M-1}$ and

$(\mathrm{S}^2 ph_{\mathrm{b}})_{M-1}$ terms, $(vib)_M$ and $(ph_{\mathrm{b}})_M$ are lumped together to give the $1\mathrm{SD}_{\mathrm{bound}}$ cross sections for the single reaction stage: (nn), (np), (pn) and (pp). These allow one to distinguish between the different sequences of the above-mentioned reaction stages that result from the $M$ collisions of the continuum nucleon with the nucleons of the target nucleus. Eq. (13) is used separately for each sequence, *e.g.* the sequences that contribute to the (p,p') reaction are the following [36]:

$1\mathrm{SD}_{\mathrm{bound}}$, (pp),
$2\mathrm{SD}_{\mathrm{bound}}$, $(\mathrm{S}^{-2}\mathrm{pp,pp}) + (\mathrm{S}^{-2}\mathrm{pn,np})$,
$3\mathrm{SD}_{\mathrm{bound}}$, $(\mathrm{S}^{-2}\mathrm{pp,S}^{-2}\mathrm{pp,pp}) + (\mathrm{S}^{-2}\mathrm{pp,S}^{-2}\mathrm{pn,np})$
$+ (\mathrm{S}^{-2}\mathrm{pn,S}^{-2}\mathrm{np,pp}) + (\mathrm{S}^{-2}\mathrm{pn,S}^{-2}\mathrm{nn,np})$,
$4\mathrm{SD}_{\mathrm{bound}}$, *etc.*

In Fig. 1, the contributions due to excitation of the one-phonon collective states *vib* and the incoherent particle–hole *ph* states are included in the 1SD cross section for the neutron scattering (nn) stage of the $^{93}$Nb(n,n')$^{93}$Nb reaction. The maximum at medium excitation energies (10÷15 MeV) in

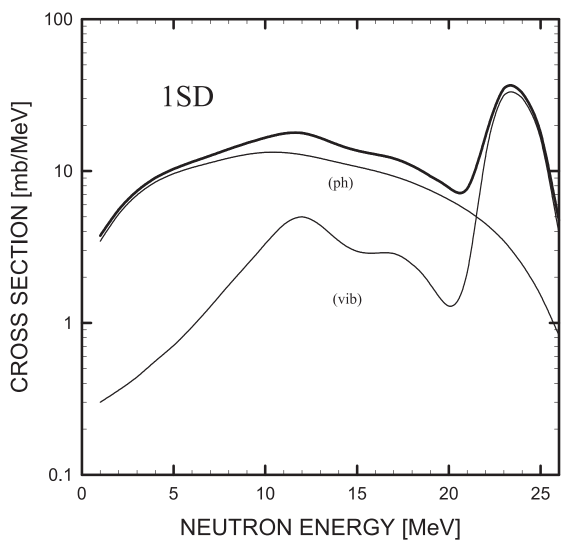


Fig. 1. The calculated 1SD cross section of the $^{93}$Nb(n,n$'$)$^{93}$Nb reaction at an incident neutron energy of 26 MeV [37], (thick solid line). The contributions due to excitation of one-phonon collective vibrations (*vib*) of multipolarity $\lambda \leq 4$ and to incoherent excitation of particle–hole-pairs (*ph*), of transferred orbital angular momenta $l>4$ are shown separately as thin lines.

Fig. 1, corresponds to the giant resonances. The structure at the highest outgoing energies is due to the individual one-phonon states described by Gaussians with a width of $\Gamma = 2$ MeV. The latter structure survives the energy smearing from the convolution of three successive neutron scattering stages, ($S^{-2}$nn, $S^{-2}$nn,nn), and appears, although weaker, as a three-phonon structure at trice higher excitation energy in the 3SD spectrum of Fig. 2. The latter figure shows the contributions of all four sequences of reaction stages. The $1\mathrm{SD}_{\mathrm{bound}} + \sum_{M>1} \mathrm{MSD}_{\mathrm{bound}}$ describe adequately the one-particle emission according to the theory of FKK. This is shown in Fig. 3, where the MSD cross sections are compared with the inclusive neutron spectrum measured at an incident energy of 25.7 MeV [38]. Fig. 3 clearly shows how the one-phonon maximum in the 1SD spectrum developes into the two-, three-, and four-phonon maxima at twice, trice and four times higher excitation energy in the 2SD, 3SD and 4SD spectra, respectively. The partial cross sections, obtained at an incident energy of 14 MeV, after integration over angle and outgoing energy, are included in Table I [39].

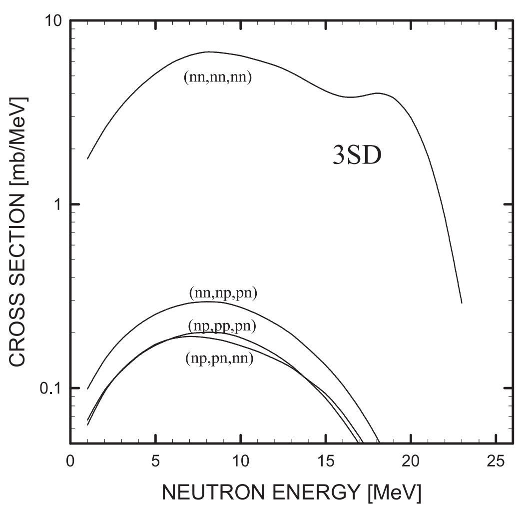


Fig. 2. The same as in figure 1 but for the 3SD. The contributions from the four sequences of reaction stage are also shown (sum of the four contributions is indistinctive from the strongest one). The enhancing factors are omitted for simplicity.

The cross sections for the $^{93}$Nb(n,xn)$^{93}$Nb reaction have also been described using the RPA basis of collective states. Due to the complexity of the calculations involved, only the first two steps of the reaction were calculated [40]. The results obtained for the 1SD and 2SD reactions are in excellent agreement with the results of [37,39] that are included in Table I. The shapes of the emission spectra in [40] also resemble the ones obtained in [37,39]. One could therefore argue that the new 1SD cross section of equations (2) through (4), in conjunction with (13), present a closed-form approximation of the RPA cross sections.

TABLE I

The decomposition of the MSD cross sections for the $^{93}$Nb(n,n')$^{93}$Nb reaction at 14 MeV, obtained with the non-normal DWBA matrix elements. The MSD reaction stages include only neutrons.

| $\sigma$(1SD) | (mb) | $\sigma$(2SD) | (mb) | $\sigma$(3SD) | (mb) |
|---|---|---|---|---|---|
| $(ph)$ | 82 | $(\mathrm{S}^{-2}vib,vib)$ | 29 | $(\mathrm{S}^{-2}vib,\mathrm{S}^{-2}vib,vib)$ | 6.8 |
| $(vib)$ | 119 | $(\mathrm{S}^{-2}vib,ph)$ | 13 | $(\mathrm{S}^{-2}vib,\mathrm{S}^{-2}vib,ph)$ | 2.0 |
| | | $(\mathrm{S}^{-2}ph,vib)$ | 9 | $(\mathrm{S}^{-2}ph,\mathrm{S}^{-2}vib,vib)$ | 1.6 |
| | | $(\mathrm{S}^{-2}ph,ph)$ | 3 | $(\mathrm{S}^{-2}vib,\mathrm{S}^{-2}ph,vib)$ | 1.2 |
| | | | | $(\mathrm{S}^{-2}ph,\mathrm{S}^{-2}vib,ph)$ | 0.3 |
| | | | | $(\mathrm{S}^{-2}vib,\mathrm{S}^{-2}ph,ph)$ | 0.2 |
| | | | | $(\mathrm{S}^{-2}ph,\mathrm{S}^{-2}ph,vib)$ | 0.2 |
| | | | | $(\mathrm{S}^{-2}ph,\mathrm{S}^{-2}ph,ph)$ | 0.03 |
| Total | 201 | | 54 | | 12.3 |

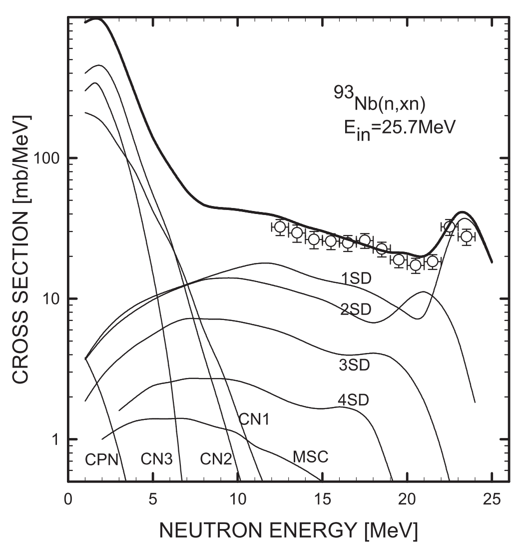


Fig. 3. Comparison of the calculated cross sections with the spectrum of neutrons from the $^{93}$Nb(n,xn)$^{93}$Nb reaction measured at incident energy of 25.7 MeV [38]. The thick line is the sum of all contributions. CN1 to CN3 denote the primary to tertiary neutrons evaporated from the compound nucleus, respectively. CPN denotes secondary neutrons preceded by evaporation of a proton and MSC labels the emission from three steps of the compound reaction.

Fig. 2 shows that in the case of neutron scattering, the sequences of reaction stages including only neutrons dominate markedly over the other ones including also protons. However, in the case of proton scattering or charge-exchange reactions one cannot foresee if and which sequences can be neglected. Therefore, all sequences are calculated and summed in order to obtain reliable MSD cross sections for the $^{54}$Fe(p,p')$^{54}$Fe and the $^{90}$Zr(p,n)$^{90}$Nb reactions considered in the following chapter. The cross sections for the sequences that contribute to the (p,n) reactions are shown in Table II [15]. For a comparison of angular distributions see [13,18,39].

TABLE II

The decomposition of the MSD cross sections for the $^{90}$Zr(p,n)$^{90}$Nb reaction at 45 MeV, obtained with the non-normal DWBA matrix elements.

| $\sigma(1\mathrm{SD})_{\mathrm{bound}}$ | (mb) | $\sigma(2\mathrm{SD})_{\mathrm{bound}}$ | (mb) | $\sigma(3\mathrm{SD})_{\mathrm{bound}}$ | (mb) |
|---|---|---|---|---|---|
| (pn) | 57 | ($S^{-2}$pn,nn) | 58 | ($S^{-2}$pn,$S^{-2}$nn,nn) | 32 |
| | | ($S^{-2}$pp,pn) | 9 | ($S^{-2}$pp,$S^{-2}$pn,nn) | 4 |
| | | | | ($S^{-2}$pn,$S^{-2}$np,pn) | 3 |
| | | | | ($S^{-2}$pp,$S^{-2}$pp,pn) | 2 |
| Total | 57 | | 67 | | 41 |
| | | | | $\sigma(4\mathrm{SD})_{\mathrm{bound}}$ | (mb) |
| | | | | ($S^{-2}$pn,$S^{-2}$nn,$S^{-2}$nn,nn) | 10.2 |
| | | | | ($S^{-2}$pn,$S^{-2}$np,$S^{-2}$pn,nn) | 1.1 |
| | | | | ($S^{-2}$pp,$S^{-2}$pn,$S^{-2}$nn,nn) | 0.9 |
| | | | | ($S^{-2}$pn,$S^{-2}$nn,$S^{-2}$np,pn) | 0.9 |
| | | | | ($S^{-2}$pp,$S^{-2}$pp,$S^{-2}$pn,nn) | 0.7 |
| | | | | ($S^{-2}$pn,$S^{-2}$np,$S^{-2}$pp,pn) | 0.4 |
| | | | | ($S^{-2}$pp,$S^{-2}$pp,$S^{-2}$pp,pn) | 0.2 |
| | | | | ($S^{-2}$pp,$S^{-2}$pn,$S^{-2}$np,pn) | 0.1 |
| Total | | | | | 15 |

## 5. The more complicated direct processes

The cross section $1\mathrm{SD}_{\mathrm{unbound}}$ to unbound particle–hole final states can be obtained by simple subtraction [15],

$$1\mathrm{SD}_{\mathrm{unbound}} = 1\mathrm{SD} - 1\mathrm{SD}_{\mathrm{bound}} = \sum_{L>4} \sigma_L(ph)_{\mathrm{unbound}} \,. \tag{14}$$

The quantity $\sigma_L(\mathrm{ph})_{\mathrm{unbound}}$ includes the difference between the state densities (7) and (6), *i.e.* $\omega_{1p_\mathrm{a}1h_\mathrm{b}}(U,\varepsilon_\mathrm{F}^\mathrm{b})-\omega_{1p_\mathrm{a}1h_\mathrm{b}}(U,B_\mathrm{a},\varepsilon_\mathrm{F}^\mathrm{b})$. The collective $\sigma_\lambda(vib)$ terms in 1SD and $1\mathrm{SD}_{\mathrm{bound}}$ cancel in $1\mathrm{SD}_{\mathrm{unbound}}$ even with the approximation assumed for the charge-exchange reactions (see Chapters 2 and 3). The $1\mathrm{SD}_{\mathrm{unbound}}$ involves processes that go beyond the scope of the FKK theory.

At incident energies below the depth of the potential well, *i.e.* below 40 MeV, $1\mathrm{SD}_{\mathrm{unbound}}$ describes the emission of one particle, followed by damping of the other continuum particle of lower energy into a final quasi-bound compound state embedded in the continuum. Such processes contribute to absorption of the flux into the n$pnh$ compound states of the A nucleus [10]. This is shown in the reaction scheme of Fig. 4 by the long solid arrows connecting the continuum $1p0h$ entrance state (in Fig. 4(a)) with the compound states (in Fig. 4(c)), via the two-particle continuum states (in Fig. 4(b)), from which only one particle (the upper short $1\mathrm{SD}_{\mathrm{unbound}}$ arrow) is emitted. These reactions complete the gradual absorption into the (n+1)$pnh$ states of the composite $(A+1)$ nucleus [5,7]. The latter transitions are shown by the long solid arrows that connect the successive continuum states (in Fig. 4(a)) with the compound states (in Fig. 4(b)). The one-step absorption into the quasi-bound $2p1h$ compound doorway state, assumed in the original FKK [2], is shown by the first l. h. s. long solid arrow.

At incident energies higher than 40 MeV, $1\mathrm{SD}_{\mathrm{unbound}}$ gives rise to the emission of two particles, since both particles of the two-particle continuum state can escape the nucleus, even after a few collisions of one of them with the bound nucleons. Thus, the two particles are emitted in a one-step or in a multistep reaction. Only simultaneous emission is important, since the alternative scenario of the emission of a secondary particle after one or a few rescattering collisions following the primary particle emission is relatively unimportant [41,42]. The double-differential $1\mathrm{SD}_{\mathrm{unbound}}$ describes the emission of one of the two emitted particles.

Although the coexistence of one-particle emission followed by damping and two-particle emission is likely to occur over a wider energy region, we assume in what follows a sharp limit of 40 MeV, for sake of clarity. Thus, only the one-step emission of two particles and the multistep rescattering processes that follow are included in $1\mathrm{SD}_{\mathrm{unbound}}$, above 40 MeV, and represented by the pairs of short arrows ($1\mathrm{SD}_{\mathrm{unbound}}$, MSD2) from the chain of the two-particle continuum states connected by the horizontal and the inclined line in Fig. 4(b). A more rigorous treatment of two-particle emission in the continuum is proposed by the theory of knock-out reactions, (a,ab), of Ciangaru [43], who has applied statistical postulates similar to those of the FKK theory. The resulting formalism has not been implemented so far in practical calculations. However, some contributions to the multistep two-particle emission and/or contributions to gradual absorption from damping that fol-

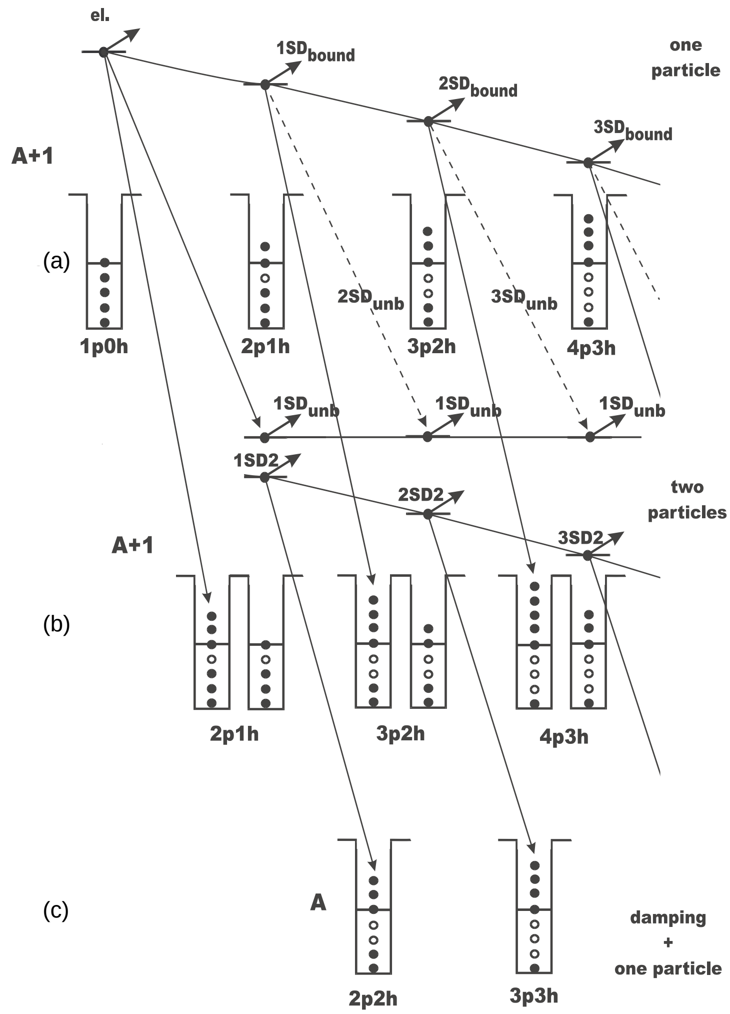


Fig. 4. Scheme of multistep direct reactions. Short arrows ($\mathrm{MSD_{bound}}$ in Fig. 4(a)) show the original multistep one-particle emission of FKK. Long solid arrows show gradual absorption of the continuum particle (if of energy lower than $\approx 40$ MeV) into quasi-bound states of the multistep compound (MSC) reaction chain (in Fig. 4(b)), except the one to the two-particle continuum state (in Fig. 4(b)), that gives rise to emission of one particle (short arrows $\mathrm{1SD_{unb}}$) followed by damping of the other one (long arrows from MSD2 to the quasi-bound states in Fig. 4(c)), or to one-step or multistep emission of two particles (pairs of short arrows, $\mathrm{1SD_{unb}}$ and MSD2), depending on energy.

lows the multistep emission of one particle (dashed arrows in Fig. 4) can be estimated in the framework of the FKK theory with the help of $\mathrm{MSD}_{\mathrm{unbound}}$ obtained by generalizing Eq. (14) to obtain $\mathrm{MSD}_{\mathrm{unbound}}=\mathrm{MSD}-\mathrm{MSD}_{\mathrm{bound}}$ [10]. The MSD cross section here, involves the convolution of $(M-1)$ enhanced $\mathrm{S}^{-2}(1\mathrm{SD}_{\mathrm{bound}})$ cross sections, just as in the convolution integral of (13). However, contrary to (13), the last $M$-th reaction step $1\mathrm{SD}_M$ is not restricted by particle binding but includes both the bound and unbound final states. On the other hand, according to the approximate method of [9], the double-differential 1SD cross section is used as input to the calculation of the cross section (1SD(2)) for the other particle in two-particle emission. This method takes no account of the influence of energy dissipation due to the rescattering collisions of the second continuum particle (1SD2, 2SD2, 3SD2,...*etc.* in Fig. 4(b)) on the 1SD(2) spectrum, although 1SD(2)=1SD2+2SD2+3SD2+... *etc.* is obeyed. Therefore, the double-differential $1\mathrm{SD}_{\mathrm{unbound}}$ and the complementary 1SD(2) determine only an approximate spectral distribution of the two particles. One has to bear in mind that according to the assumption of a sharp 40 MeV limit, the integrated $1\mathrm{SD}_{\mathrm{unbound}} = 1\mathrm{SD}(2)$ above 40 MeV. Here the two sides of the equation may include nucleons of different kind, *e.g.* in case of a (p,n) reaction the (p,np) two-particle emission may follow. However, only nucleons of the same kind (neutrons in this case) are compared with experiment and this involves two source reactions, the (p,n) and the (p,p') with the latter contributing via the (p,pn) two-particle emission. The $1\mathrm{SD}_{\mathrm{unbound}}$, integrated over angle and energy, gives the total cross section for two-particles in the continuum. The latter increases with increasing energy, although in the case of a (p,n) reaction it remains practically constant compared to the total one-particle emission cross section of FKK (integrated $1\mathrm{SD}_{\mathrm{bound}} + \sum_{M>1}\mathrm{MSD}_{\mathrm{bound}}$). This is shown in Table III for the $^{90}$Zr(p,n)$^{90}$Nb reaction [10]. The total one-particle emission amounts to approximately 65% (third row) of the direct reactions, independent of the incident energy. The remaining 35% (fourth and fifth rows) corresponds to the $1\mathrm{SD}_{\mathrm{unbound}}$, which is one-particle emission associated with damping of the other continuum particle at low incident energies, but with increasing energy it includes increasingly more two-particle emission. It thus turns out, that 35% of the total (p,n) reaction cross section corresponding to the more complicated direct processes is not accounted for in the FKK theory.

Nucleon scattering is different. The slowly varying contribution from the collective isoscalar vibrations to $1\mathrm{SD}_{\mathrm{bound}}$ (Eq. (3)), increases the one-particle emission of the FKK theory considerably. The $1\mathrm{SD}_{\mathrm{bound}}$ cross section itself becomes two to three times greater than the one for a charge-exchange reaction (compare the first rows in Tables III and IV). This makes one-particle emission dominant at incident energies below $\approx 40$ MeV and

TABLE III

The integrated cross sections for the $^{90}$Zr(p,n)$^{90}$Zr reaction including the enhanced $MSD_{bound}$ contributions calculated with the non-DWBA matrix elements. The cross sections are verified by comparison with experiment as in Figs. 7 and 8 and given in mb.

| Incident energy | 25 MeV | 45 MeV | 80 MeV | 120 MeV | |
|---|---|---|---|---|---|
| Cross section | | | | | Emission |
| $1SD_{bound}$ | 60 | 57 | 34 | 24 | one particle |
| $MSD_{bound}$ | 13 | 123 | 456 | 355 | one particle |
| $\sum_{M\geq 1} MSD_{bound}$ | 73 | 180 | 490 | 379 | one particle |
| $1SD_{unbound}$ | 39 | | | | one particle + damping |
| $1SD_{unbound}$ | | 89 | 199 | 232 | two particles |

TABLE IV

The integrated cross sections for the $^{54}$Fe(p,p')$^{54}$Fe reaction including the enhanced $MSD_{bound}$ contributions calculated with non-DWBA matrix elements. The cross sections are verified by comparison with experiment as in Figs. 5 and 6, and given in mb.

| Incident energy | 29 MeV | 39 MeV | 62 MeV | |
|---|---|---|---|---|
| Cross section | | | | Emission |
| $1SD_{bound}$ | 118 | 116 | 108 | one particle |
| $MSD_{bound}$ | 69 | 164 | 267 | one particle |
| $\sum_{M\geq 1} MSD_{bound}$ | 187 | 280 | 375 | one particle |
| $1SD_{unbound}$ | 16 | 40 | | one particle + damping |
| $1SD_{unbound}$ | | | 92 | two particles |

allows one to conclude that nucleon scattering at low energies is the principal field of application of the FKK theory. At higher energies, the increase of one-particle emission to bound final states is compensated by the fast increase of $1SD_{unbound}$. As can be seen in Table IV already at 62 MeV the $1SD_{unbound}$ rises to 20% (fifth row) of the total flux involved (fourth or fifth plus third rows).

In Figs. 5 through 8, the calculated cross sections are compared with experimental data. The cut-off of the low-energy part of the $1SD_{bound}$ spectra is a result of considering only bound final $1p1h$ states. Hence, the $1SD_{bound}$ spectra extend over a constant energy interval that is approximately equal to the depth of the nuclear potential well and therefore, observe the EWSR's limits independent of incident energy. At incident energies below 30 MeV, only 1SD and 2SD cross sections are important for the charge-exchange (p,n) reactions. The 3SD contribution appears non-negligible for nucleon scattering. On the other hand, at the highest energies of 80–120 MeV, up to 6SD–8SD cross sections are important. At 120 MeV, the MSD cross sections appear to converge only at the 7th reaction stage, as is shown in Fig. 8.

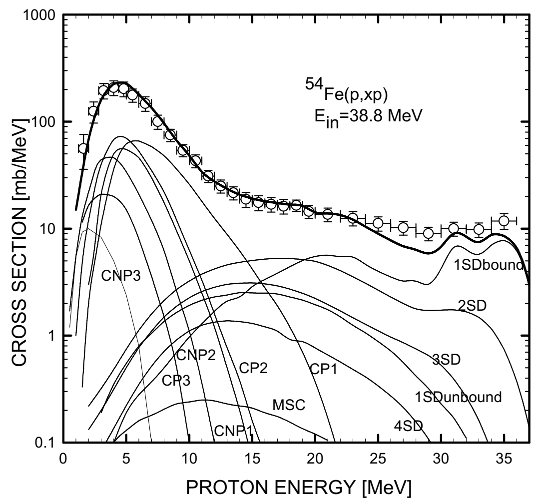


Fig. 5. Comparison of the MSD cross sections calculated with the non-DWBA matrix elements with inclusive spectrum of protons from the $^{54}$Fe(p,xp)$^{54}$Fe reaction, measured at 38.8 MeV [44]. The thick line is the sum of all contributions. CP1 to CP3 are protons evaporated successively from the compound nucleus. CNP1 to CNP3 denote successive protons preceded by evaporation of a neutron and MSC labels the sum of emissions from three steps of the pre-equilibrium compound reaction. The 1SD cross section is split into the $1SD_{\rm bound}$ and $1SD_{\rm unbound}$ components. Only the former are folded into the MSD cross sections.

The cross sections for multiple evaporation of nucleons from the compound nucleus are calculated according to the theory of Hauser and Feshbach. The multistep compound (MSC) reaction cross sections are calculated in the framework of the FKK theory [2,5], allowing for a gradual absorption of incident flux into the quasi-bound (n+1)$p$n$h$ states of the MSC reaction chain [5]. The radial overlap integral of the single-particle wave functions in the MSC cross section is calculated with constant wave functions within the nuclear volume. The overlap integral was subsequently reduced by 0.5 in order to approximate the result of the microscopic calculation [47]. The resulting cross sections constitute thus about 0.25 of those

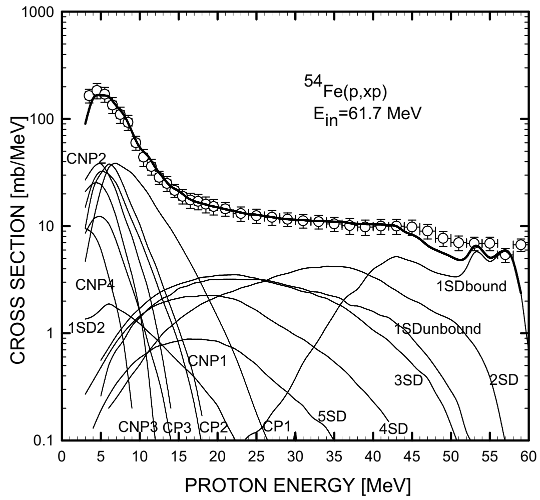


Fig. 6. The same as in Fig. 5 but at incident energy of 61.7 MeV [44].

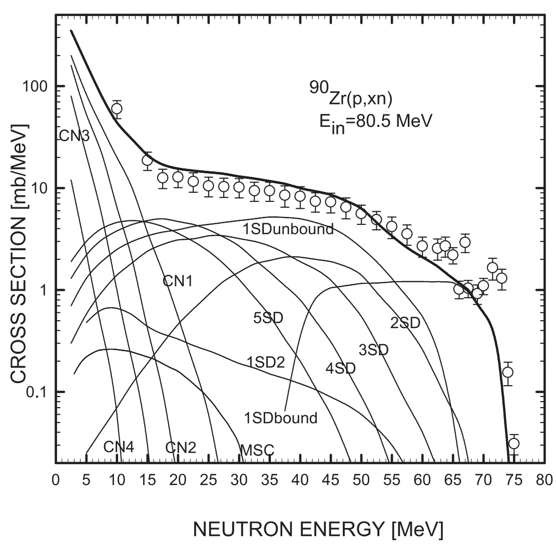


Fig. 7. Comparison of the calculated cross sections with neutrons emitted from the $^{90}$Zr(p,xn)$^{90}$Nb reaction measured at incident energy of 80 MeV [45]. The thick line is a sum of all contributions shown. The labels CN1 to CN4 denote successive neutrons evaporated from the compound nucleus, respectively. MSC labels the sum of emissions from the three steps of the preequilibrium compound reaction. The 1SD cross section is split into the $1SD_{\rm bound}$ and $1SD_{\rm unbound}$ components. Only the former ones are folded into the MSD cross sections [15].

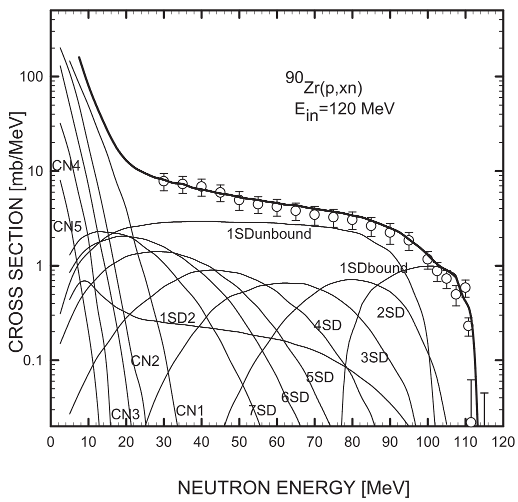


Fig. 8. The same as in Fig. 7 but at incident energy of 120 MeV [46]. The MSD cross sections converge only at the 7SD stage [15].

obtained in standard analyses. The MSC cross sections are non-negligible only at low incident energies. However, even at energies below 30 MeV, the MSC component plays no significant role in comparison with the MSD one. This is partly due to the reduced microscopic radial overlap integral and partly due to the gradual absorption, which by feeding directly the compound states of increasing complexity weakens the usually strong 1SC emission from the quasi-bound $2p1h$ state. The optical model absorption cross section that feeds the compound nucleus is appropriately reduced to account for the direct non-elastic reactions considered [12].

In all the above described calculations, the optical potentials of [48] and [49,50] were used for low-energy neutrons and protons, respectively. At energies above 50 MeV, the optical potentials of [51,52] were used for neutrons and those of [50,51] for protons.

## 6. Conclusions

The MSD cross sections calculated in the framework of the FKK theory, using (*i*) the $1\mathrm{SD}_{\mathrm{bound}}$ cross sections to bound final states of Eq. (2) [10,15] and (*ii*) the enhanced non-DWBA matrix elements in the convolution integral (13) are able to reproduce the cross sections of nucleon-induced reactions very well without resorting to free parameters. Although at very low incident energies, *e.g.* at 14 MeV, the convolution of the 1SD cross sections (including bound and unbound final states) instead of the $1\mathrm{SD}_{\mathrm{bound}}$ cross sections makes little difference, in a rigorous approach the 1SD cross sections cannot be considered as genuine one-step cross sections since they involve a low energy unbound particle in the final state, which undergoes preferably damping transitions. On the other hand, $1\mathrm{SD}_{\mathrm{bound}}$ is a well defined one-step one-particle cross section that observes the EWSR's limits, independent of incident energy. Using the smoothed enhancing factors $\langle \mathrm{S}_L^{-1} \rangle$ in the non-DWBA matrix elements together with the restricted $1\mathrm{SD}_{\mathrm{bound}}$ cross sections enables us to avoid the divergence of MSD cross sections at energies above 50 MeV [15,36,53]. The average enhancement of the MSD cross sections with respect to the normal DWBA ones is $(3.5\text{–}3.9)^{M-1}$, almost independent of the type of reaction and incident energy [15].

The $1\mathrm{SD}_{\mathrm{unbound}}$ describes either the emission of one particle followed by damping transitions of the other continuum particle at lower energies or the emission of two particles. Thus, multistep two-particle emission just like the multistep one-particle emission of FKK, is accompanied by gradual absorption of the continuum nucleons into the quasi-bound states that develop towards the equilibration of the compound $A$ and $(A+1)$ nuclei [5,7,10], respectively.

The author acknowledges the long-lasting fruitful cooperation of Drs. P. Demetriou and B. Mariański.

## REFERENCES

[1] M. Blann, *Ann, Rev. Nucl. Sci.* **25**, 123 (1975).

[2] H. Feshbach, A. Kerman, S.E. Koonin, *Ann. Phys.* (*N.Y.)* **125**, 429 (1980).

[3] T. Tamura, T. Udagawa, H. Lenske, *Phys. Rev.* **C26**, 379 (1982).

[4] H. Nishioka, H.A. Weidenmüller, S. Yoshida, *Ann. Phys.* (*N.Y.)* **183**, 166 (1988).

[5] A. Marcinkowski, J. Rapaport, R.W. Finlay, C. Brient, M. Herman, M.B. Chadwick, *Nucl. Phys.* **A561**, 387 (1993).

[6] M.S. Hussein, R. Bonetti, *Phys. Lett.* **B112**, 13 (1982).

[7] G. Arbanas, M.B. Chadwick, F.S. Dietrich, A. Kerman, *Phys. Rev.* **C51**, R1078 (1995).

[8] H. Nishioka, H.A. Weidenmüller, S. Yoshida, *Z. Phys.* **A336**, 197 (1990); *J. Phys.* **193**, 195 (1989).

[9] M.B. Chadwick, P.G. Young, D.C. George, Y. Watanabe, *Phys. Rev.* **C50**, 996 (1994).

[10] A. Marcinkowski, P. Demetriou, *Eur. Phys. J.* **A21**, 287 (2004).

[11] A. Marcinkowski, B. Mariański, *Phys. Lett.* **B433**, 223 (1998).

[12] A. Marcinkowski, B. Mariański, *Nucl. Phys.* **A653**, 3 (1999).

[13] A. Marcinkowski, P. Demetriou , B. Mariański, *Nucl. Phys.* **A694**, 312 (2001); *APH N.S., Heavy Ion Phys.* **16/1-4**, 35 (2002).

[14] H. Kalka, M. Torjman, D. Seeliger, *Phys. Rev.* **C40**, 619 (1989).

[15] P. Demetriou, A. Marcinkowski, *Nucl. Phys.* **A714**, 75 (2003); also in *Proc. 10th Int. Conf. on Nuclear Reaction Mechanisms*, ed. E. Gadioli, Varenna 2003, Universitá degli studi di Milano, Supplemento N. 122, p. 331.

[16] G.A. Needham, F.P. Brady, D.H. Fitzgerald, J.L. Romero, J.L. Ullman, J.W. Watson, C. Zanelli, N.S.P. King, G.R. Satchler, *Nucl. Phys.* **A385**, 349 (1982).

[17] A. van der Woude, in: J. Speth (Ed.) *Electric and Magnetic Giant Resonances in Nuclei*, World Scientific, Singapore 1991, pp. 177, 214.

[18] P. Demetriou, A. Marcinkowski, B. Mariański, *Nucl. Phys.* **A697**, 171 (2002).

[19] S.M. Austin, in: C.D. Goodman, *et al.* (Eds.), *Proc. Conf. on (p,n) Reactions and the Nucleon–Nucleon Force*, Telluride, Colorado 1979, Plenum Press, N.Y. 1980, p. 203.

[20] E. Gadioli, P.E. Hodgson, *Pre-equilibrium Nuclear Reactions*, Clarendon, Oxford 1992, p. 385.

[21] M. Hilman, J.R. Grover, *Phys. Rev.* **185**, 1303 (1969).

[22] P.D. Kunz, E. Rost, in: K. Langanke *et al.* (Eds.), *Computational Nuclear Physics,* Vol. 2, Springer, Berlin 1993, Ch. 5.

[23] C.Y. Fu, *Nucl. Sci. Eng.* **92**, 440 (1986).

[24] P. Oblozinsky, *Nucl. Phys.* **A453**, 127 (1986).

[25] A.J. Koning, M.B. Chadwick, *Phys. Rev.* **C56**, 970 (1997).

[26] E. Betak, J. Dobes, *Z. Phys.* **279**, 319 (1976).

[27] R. Bonetti, M. Camnasio, L. Colli-Milazzo, P.E. Hodgson, *Phys. Rev.* **C24**, 71 (1981).

[28] G.R. Satchler, *Direct Nuclear Reactions*, Clarendon, Oxford 1983.

[29] S. Tsai, G.F. Bertsch, *Phys. Lett.* **B73**, 247 (1978).

[30] S. Yoshida, presented at Workshop on Open Problems in Quantum-Mechanical Approaches to Multistep Direct Nuclear Reactions, held at ECT, Trento, Italy, July 27-August 1, 1998.

[31] A. Marcinkowski, R.W. Finlay, J. Rapaport, P.E. Hodgson, M.B. Chadwick, *Nucl. Phys.* **A501**, 1 (1989).

[32] N.A. Smirnova, N. Pietralla. T. Mizusaki, P. Van Isacker, *Nucl. Phys.* **A678**, 235 (2000).

[33] I. Kumabe, M. Haruta, M. Hyakutake, M. Matoba, *Phys. Lett.* **B140**, 272 (1984).

[34] H. Feshbach, *Ann. Phys. (N.Y.)* **159**, 150 (1985).

[35] P. Demetriou , A. Marcinkowski, B. Mariański, *Phys. Lett.* **B493**, 28 (2000).

[36] P. Demetriou, A. Marcinkowski, B. Mariański, *Nucl. Phys.* **A707**, 354 (2002).

[37] A. Marcinkowski, P. Demetriou, *Acta Phys. Pol. B* **35**, 767 (2004); also in *Proc. 10th Int. Conf. on Nuclear Reaction Mechanisms*, ed. E. Gadioli, Varenna 2003, Universitá degli studi di Milano, Supplemento N. 122, p. 321.

[38] A. Marcinkowski, R.W. Finlay, G. Randers-Pehrson, C.E. Brient, R. Kurup, S. Mellema, A. Meigooni, R. Tailor, *Nucl. Sci. Eng.* **83**, 13 (1983).

[39] P. Demetriou, A. Marcinkowski, B. Mariański, *Acta Phys. Pol. B* **32**, 3003 (2001).

[40] H. Lenske, H.H. Wolter, M. Herman, G. Reffo, in *Proc. 7-th Int. Conf. on Nuclear Reaction Mechanisms*, ed. E. Gadioli, Varenna 1994, Universitá degli studi di Milano, Supplemento N. 100, p. 110.

[41] M. Blann, H. Vonach, *Phys. Rev.* **C28**, 1475 (1983).

[42] M.B. Chadwick, Los Alamos National Laboratory Document LA-UR-92-2346, 1992, unpublished.

[43] G. Ciangaru, *Phys. Rev.* **C30** 479 (1984).

[44] F.E. Bertrandt, R.W. Peelle, *Phys. Rev.* **C8**, 1045 (1973).

[45] M. Blann, R.R. Doering, A. Galonsky, D.M. Patterson, F.E. Serr, *Nucl. Phys.* **A257**, 15 (1976).

[46] M. Trabandt, *Thesis*, Universität Hamburg, 1989.

[47] T. Kawano, *Phys. Rev.* **C59**, 865 (1999); and private communication.

[48] D. Wilmore, P.E. Hodgson, *Nucl. Phys.* **55**, 673 (1964).

[49] F.D. Becchetti, G.W. Greenless, *Phys. Rev.* **182**, 1190 (1969).

[50] F. Björklund, in: *Proc. of Int. Conf. on Nuclear Optical Model*, Tallahassee Fl, 1959, *The Florida State University Studies*, **No. 32**.

[51] D.G. Madland, in: B. Strohmaier (Ed.),*Proc. of Specialists Meeting on Pre-equilibrium Reactions*, Semmering, Austria, 1988, OECD Paris, 1988, p. 197.

[52] R.L. Walter, P.P. Guss, in: P.G. Young (Ed.), *Nuclear Data for Basic and Applied Science*, Santa Fe NM, 1985, Gordon & Breach, New York 1986, p. 1079.

[53] M.B. Chadwick, P.G. Young, F.S. Dietrich, Lawrence Livermore National Laboratory Report UCRL-JC-117460, June 1994.